Arch. Metall. Mater. **70** (2025), 1, 87-96

DOI: https://doi.org/10.24425/amm.2025.152509

S. SATHISH[1*], V. ANANDAKRISHNAN[2], M. GUPTA[3]

INVESTIGATIONS ON THE WEAR BEHAVIOUR AND MECHANISM OF Mg-3Al/5.6Ti COMPOSITE UNDER DRY SLIDING

Magnesium containing 3 weight percentages of aluminium particles and 5.6 weight percentages of titanium particles (reinforcement) was prepared using the disintegrated melt deposition technique to investigate their synergistic effect on the tribological behaviour of Mg-3Al/5.6Ti composite. Metallographic features of the composite samples were analysed using x-ray diffraction analysis and scanning electron microscopy to disseminate the particle distribution and phase formation. The wear behaviour of the samples was studied using dry sliding wear testing by systematically varying load and sliding velocity over a sliding distance of 2000 m. The post-failure analysis was performed on the worn surface of pins, and the collected debris using scanning electron microscopy and the mechanisms involved in the wear behaviour of composite samples were identified.

Keywords: Metal-metal composite; magnesium composite; dry sliding; wear mechanism; debris analysis

1. Introduction

Magnesium-based alloys and composites are the most preferred eco-friendly material and find extensive applications in many industries, including automotive, aerospace, marine, biomedical and defence sectors, due to their lightweight, high specific stiffness and good damping capacity [1-3]. The replacement of existing components with magnesium composites directly helps in the reduction of weight and carbon emission. The major automotive components include the steering, wheel, transmission, and engine parts. However, owing to its lower strength and instability at high temperatures, the usage of pure magnesium is limited, which in turn primes the making of magnesium alloys [4] and composites with particulate reinforcements. Aluminium, copper, nickel, and silicon are some common alloying elements added to magnesium to enhance its characteristics [5-8]. Among the various magnesium alloys available, AM (Mg-Al-Zn) are the magnesium alloy series with a higher weight percentage of aluminium as an alloying element [9].

Further, the major challenge in using magnesium based materials in engineering industries is their resistance to wear, which can be addressed by understanding their tribological behaviour [10]. Likewise, identifying the tribological response of magnesium-based materials, including composites, provides a clear idea of their usage, and further, it is helpful during the replacement of existing materials. Various researchers have already conducted much research to explore their tribological behaviour in line with the progress in synthesising newer magnesium-based materials. Taltavull et al. investigated the tribological behaviour of magnesium alloy (AM50B) with the dry sliding wear test and identified the wear mechanisms under different conditions [11]. Similarly, the wear behaviour of magnesium alloys Mg97Zn1Y2 [12], and Mg-Si [10] was studied, and the wear mechanisms that influence the wear rate were identified and reported. The effect of the addition of magnesium on the wear behaviour of functionally graded composite was investigated, and observed a considerable improvement in the wear resistance on the composite [13]. Based on the investigations on the dry sliding wear of magnesium alloy AZ31B, Srinivasan et al. reported that the wear rate decreased with an increase in sliding speed due to the formation of oxide film [14]. Seenuvasaperumal et al. investigated the tribological behaviour of the squeeze-cast magnesium alloy with and without calcium hexaboride and identified the primary wear mechanisms responsible for wear [15]. The tribological behaviour of magnesium alloy Mg-3Al-0.4Si-0.1Zn was investigated at different combinations of load and temperature, and the effect of parameters on the wear mechanisms was studied [16]. Investigations on the effect of the

[1] ANNA UNIVERSITY, DEPARTMENT OF PRODUCTION TECHNOLOGY, MADRAS INSTITUTE OF TECHNOLOGY CAMPUS, CHENNAI-600044, TAMIL NADU, INDIA
[2] DEPARTMENT OF PRODUCTION ENGINEERING, NATIONAL INSTITUTE OF TECHNOLOGY TIRUCHIRAPPALLI-620015 TAMIL NADU, INDIA
[3] NATIONAL UNIVERSITY OF SINGAPORE (NUS), DEPARTMENT OF MECHANICAL ENGINEERING, 9 ENGINEERING DRIVE 1, SINGAPORE 117576, SINGAPORE

* Corresponding author: sadish.kss@gmail.com

wear behaviour of magnesium alloy Mg-3Al-0.4Si were carried out at different combinations of load and sliding velocity, and the results explored the mild and severe wear regimes in the wear map [17]. Investigations on the mechanical and wear behaviour of magnesium alloy Mg-Al-Zn were carried out, and the dominant wear mechanisms were identified as abrasion, oxidation and delamination [18]. Investigations on the wear behaviour of magnesium alloy Mg-3Al-3Sn were carried out at two different loads, and a reduction of wear rate with an increase in strontium addition was observed [19]. Investigations on the wear behaviour of magnesium composite produced through powder metallurgy were carried out, and the delamination and deformations were observed on the worn surface of composites [20]. Based on the earlier research on the tribological behaviour of magnesium and its alloys, an in-depth investigation of the tribological behaviour and a detailed study of the wear mechanisms is found essential for every material synthesised. Considering the potential of disintegrated melt deposited Mg-3Al/5.6Ti metal-metal composite, the present work primarily aims to investigate its tribological behaviour with a more specific and in-depth analysis of various wear mechanisms exhibited during dry sliding wear tests.

2. Experimental Details

2.1. Material synthesis

Aluminium (>98% purity; Alfa Aesar) and Titanium powders (>98% purity; Merck) with particle sizes less than 140 micrometres and 15 micrometres, respectively, were used to produce Mg-3Al/5.6Ti metal-metal composite [4,6]. Magnesium (>99.9% purity; ACROS Organics, USA) and the required amount of aluminium and titanium were heated to 750°C in a graphite crucible under a controlled argon environment. The melt was intermittently stirred at 460 rpm with a Zirtex 25-coated steel twin-blade stirrer for 5 minutes to attain the uniform distribution of elements. Then, the melt was allowed to pour through an orifice with a diameter of 10 mm, and it disintegrated with two argon gas jets [4]. The disintegrated melt was allowed to solidify to obtain an ingot of 40 mm in diameter. Next, the ingot was machined to a dimension of 36 mm diameter, and it was soaked at a temperature of 400°C for one hour in an electric furnace under an argon environment. Then, it is hot extruded with an extrusion ratio of 20.25:1, and the composite was obtained as cylinders with an 8 mm diameter. From the extruded magnesium metal-metal composite, samples were cut, polished and etched with Nital solution to obtain the microstructure and subsequently immersed in a solution mixture of 10 ml HF and 90 ml H_2O mixture to darken the $Mg_{17}Al_{12}$ as per ASM standard [21]. Then, the samples were subjected to metallographic examinations, namely Rigaku Ultima III XRD x-ray diffraction analysis, Carl Zeiss Gemini SEM S300H scanning electron microscopic analysis, and the energy dispersive spectroscopy analysis. From the extruded Mg-3Al/5.6Ti metal-metal composite, cylindrical pin samples of 8 mm diameter and 20 mm height were also sectioned for wear tests. The sliding end of the pins and the surface of the counterpart disc were polished using a Bainpol variable speed double disc polishing machine to obtain a uniform surface roughness of less than 0.5 micrometres.

2.2. Wear test

As per ASTM G99 standards, dry sliding wear tests were performed on a Ducom Pin-on-Disc tribometer using EN 31 die steel as a counterpart. Wear tests were performed on the samples by varying the sliding velocity (1, 2 and 3 m/s) and applied load (9.81, 19.62 and 29.43 N) for a constant sliding distance of 2000 m [22,23]. The pressure corresponding to the applied 9.81, 19.62 and 29.43 N is 0.1952, 0.3903 and 0.5855 N/mm^2, respectively. During the wear tests, the amount of wear, frictional force and coefficient of friction were recorded using a computerised data acquisition system. After dry sliding wear tests, with different combinations of load and sliding velocity over a constant sliding distance, the wear of magnesium metal-metal composite was obtained in the linear wear measures, as it is more precise compared with the weighing method [24]. Then, the obtained wear in the linear measure is converted to wear rate with appropriate geometric relation, as shown in equation (1) [25-27].

$$Wear\ rate\ (\mathrm{mm}^3/\mathrm{m}) = \frac{\left(\frac{\pi}{4} * Diameter\ of\ pin^2 * Linear\ wear\ in\ pin\right)}{Sliding\ distance} \quad (1)$$

3. Results and discussion

3.1. Metallurgical analysis

The magnesium metal-metal composite (Mg-3Al/5.6Ti) comprises aluminium and titanium. The possible intermetallic phase formation due to adding aluminium and titanium are $Mg_{17}Al_{12}$, Mg_2Al_3, AlTi, Al_2Ti, Al_3Ti, Ti_2Al, and Ti_3Al. When considering the free energy required to form these intermetallic phases, the free energy formation for $Mg_{17}Al_{12}$ is lower than the other phases [4]. Fig. 1 displays the peaks of the magnesium metal-metal composite observed from the x-ray diffraction analysis. The observed peaks were annotated as shown, displaying the peaks relevant to magnesium and titanium. Besides the peaks, relevance to the phase $Mg_{17}Al_{12}$ is observed, resulting from the reaction of added aluminium with magnesium. The higher peak intensity is observed for magnesium due to its higher concentration. At the same time, titanium and phase $Mg_{17}Al_{12}$ intensities are observed to be lesser than magnesium. Fig. 2 shows the microstructure of the produced magnesium metal-metal composite with titanium in the form of particles and needles. Also, intermetallic $Mg_{17}Al_{12}$ is observed in the microstructure (Enlarged view inside Fig. 2), which is confirmed by the spectrum analysis inside Fig. 2. The estimated free energy

formation of the intermetallic $Mg_{17}Al_{12}$ is lesser than that of other intermetallics like Al3Ti. Thus, the addition of aluminium in the liquid processing helps in the $Mg_{17}Al_{12}$ intermetallic formation. Similar findings of $Mg_{17}Al_{12}$ intermetallic formation due to the addition of aluminium are observed elsewhere [4,28-30]. From the energy dispersive spectroscopy analysis, the elemental maps were attained for the produced magnesium composite as shown in Fig. 3a-c. Fig. 3a shows the SEM image of the magnesium composite corresponds to the EDS analysis. Fig. 3b shows the map corresponding to the magnesium, where the entire region of

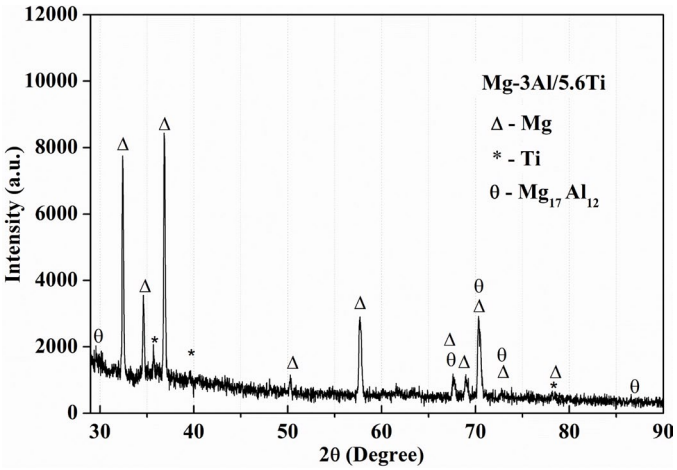

Fig. 1. X-Ray diffraction analysis of Mg-3Al/5.6Ti

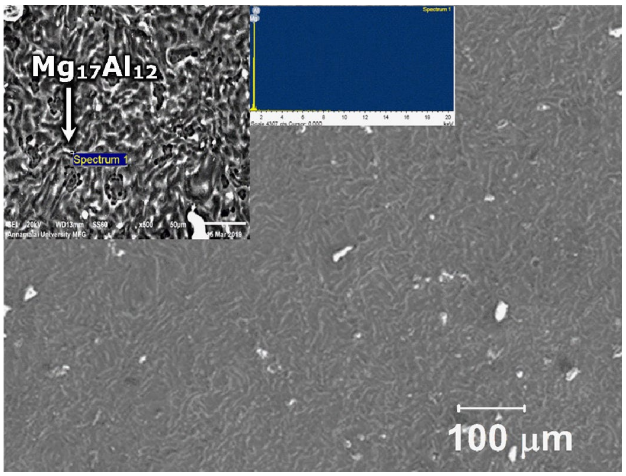

Fig. 2. Scanning electron microscope image of Mg-3Al/5.6Ti

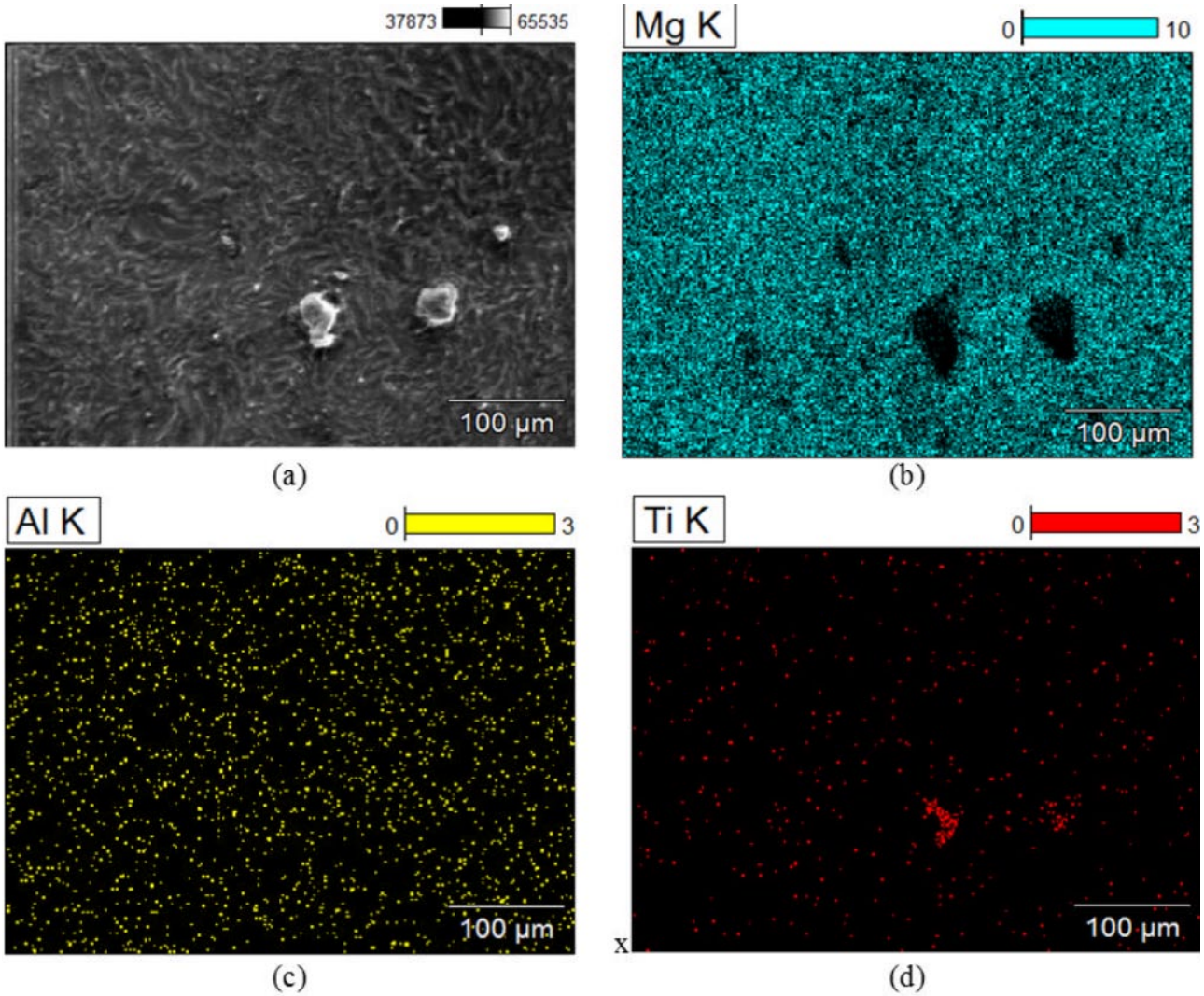

Fig. 3. Elemental mapping of Mg-3Al/5.6Ti with elements of (a) SEM image (b) Magnesium (c) Aluminium (d) Titanium

the map is filled with a few voids (appearing in black). Fig. 3c shows the map corresponding to the aluminium, which shows the uniform distribution of added elements. Fig. 3d shows the map corresponding to the titanium in which clusters of red spots are observed, and the same is matched with the void region of the magnesium element map. As the aluminium is mutually soluble with the magnesium matrix, it is shown as fully dispersed, whereas the titanium was retained as it is in the matrix due to its insolubility with magnesium. Thus, the elemental maps confirm the presence of magnesium, aluminium and titanium particles.

3.2. Wear analysis

The wear behaviour of magnesium metal-metal composite is analysed by plotting the wear rate of the composite against the sliding distance for the different loads and sliding velocities. The wear rate for a 9.81 N load with different sliding velocities is shown in Fig. 4; at 1 m/s sliding velocity, a little reduction in wear rate is observed with an increase in sliding distance. Whereas, at 2 m/s and 3 m/s sliding velocities, a higher wear rate is observed at the initial stages (i.e., 500 m sliding distance), and a further increase in the sliding distance leads to the reduction of wear rate. The reason is that the pressure acting on the surface is lower at lower loads, and the surface contact is at asperity levels. The wear rate of magnesium metal-metal composite at different sliding velocities for 19.62 N and 29.43 N load is shown in Figs. 5 and 6. A higher wear rate is observed at a lower sliding velocity of 1 m/s, and a lower wear rate is observed at a higher sliding velocity of 3 m/s in 19.62 N and 29.43 N loading conditions. At all loads, an increase in sliding velocity results in the reduction of wear rate; this is due to the formation of oxide layers between the contact surface and the same is observed in the worn surface and wear debris analysis. Similar findings of the formation of oxide layers at increased sliding velocity on the wear pins were reported by Turan et al. and Zhang et al. [31,32]. When comparing the wear rate of pure magnesium (from literature) [33-35] with the wear rate of magnesium metal-metal composite, the wear rate is found to be high for pure magnesium and less for magnesium metal-metal composite. The reason is due to the addition of titanium and the formation of intermetallic phase $Mg_{17}Al_{12}$ (as observed in XRD (Fig. 1) and SEM image (Fig. 2)). The addition of aluminium and titanium in the developed Mg-3Al/5.6Ti composite improved the hardness value from 48 HV (Pure Magnesium) to 78 HV, along with the grain refinement reported by Sankaranarayanan et al. [4].

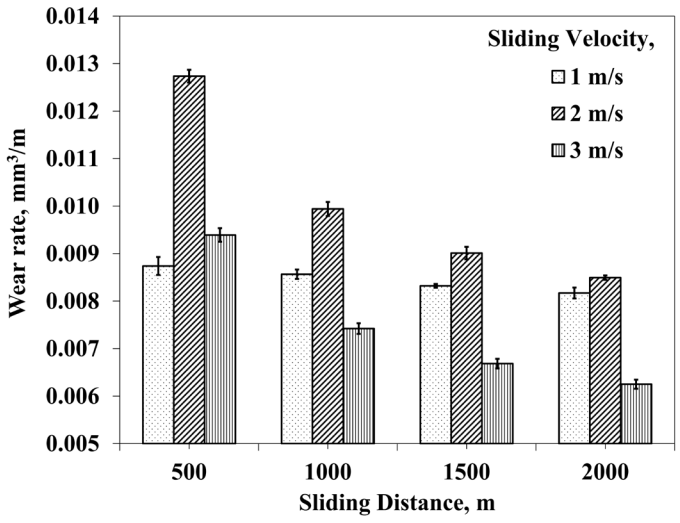

Fig. 4. Wear rate with respect to varying sliding velocity at 9.81 N load

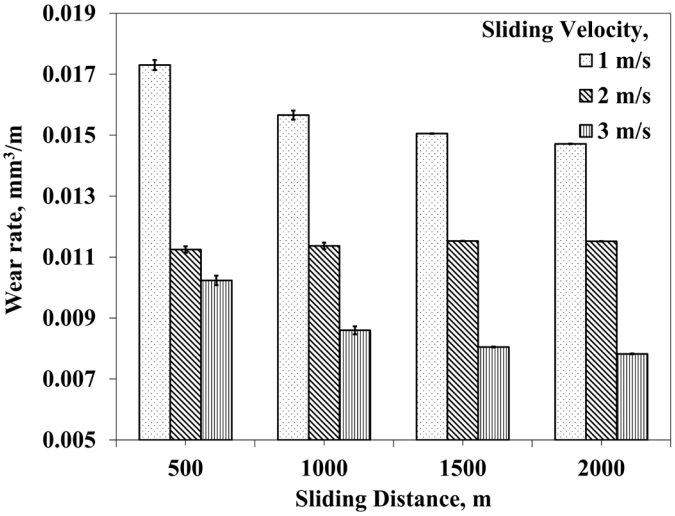

Fig. 5. Wear rate with respect to varying sliding velocity at 19.62 N load

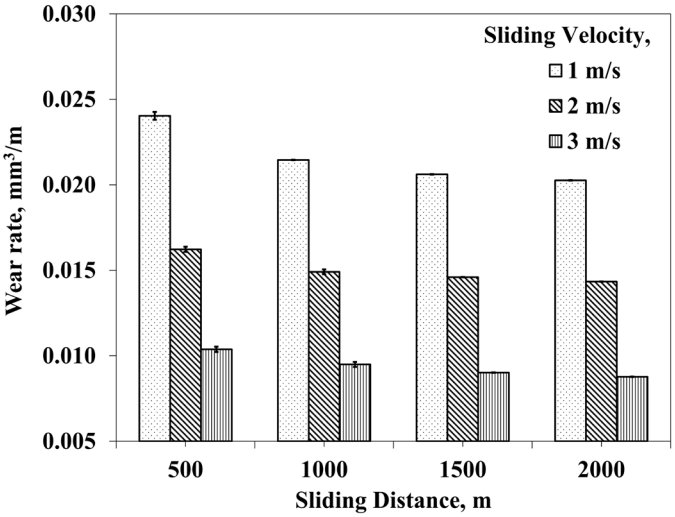

Fig. 6. Wear rate with respect to varying sliding velocity at 29.43 N load

The coefficient of friction at 9.81 N load for different sliding velocities is shown in Fig. 7. At 1 m/s sliding velocity and 500 m sliding distance, the coefficient of friction is found to be higher, and then it decreases with the increase in sliding distance. As the contact between the sliding pairs is at asperity levels, the coefficient of friction at the initial stages is found to be higher. Further, an increase in sliding results in the reduction of the coefficient of friction due to the nonlinearity of the contact area, as reported by Shizhu and Ping [36]. At 2 m/s and 3 m/s sliding velocities,

the coefficient of friction is found to be slightly reduced with an increase in sliding distance, and this is due to the formation of a thin oxide film layer between the contact surface at higher velocities. The coefficient of friction at 19.62 N load for different sliding velocities is shown in Fig. 8. At all sliding velocities, the coefficient of friction is found to be slightly reduced with an increase in sliding distance. The coefficient of friction at 29.43 N load for different sliding velocities is shown in Fig. 9. At all sliding velocities, the coefficient of friction is higher at the initial sliding stages and a further increase in sliding distance results in the reduction of the coefficient of friction. As said earlier, at the initial stages, the contact is at asperity levels, the coefficient of friction is higher and further sliding of the pin results in a uniform area of contact. Almost in all the conditions, the lowest coefficient of friction is observed at lower loads and lower sliding velocity, and this is due to the minimum force acting on the pin at lower loading conditions. It is obvious that the frictional force has direct kinetics with the applied load, induces the plastic deformation of the surface, and results in the variation of the actual area of contact as observed elsewhere [37-41].

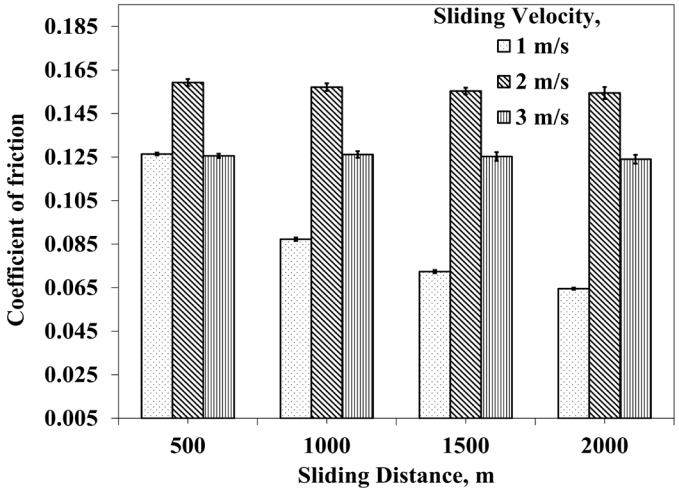

Fig. 7. Coefficient of friction with respect to varying sliding velocity at 9.81 N load

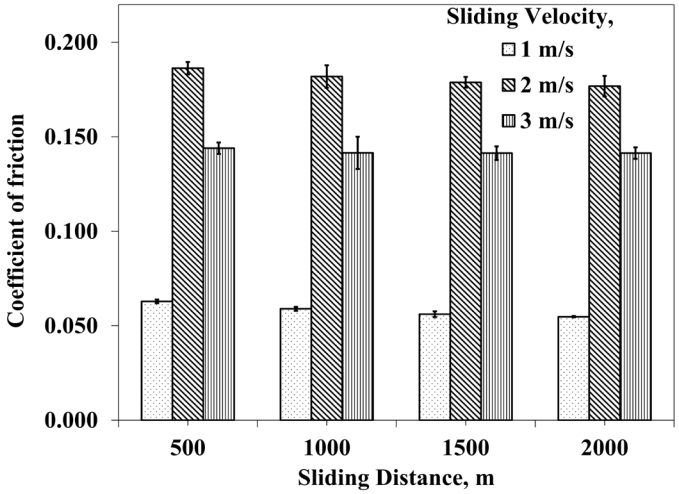

Fig. 8. Coefficient of friction with respect to varying sliding velocity at 19.62 N load

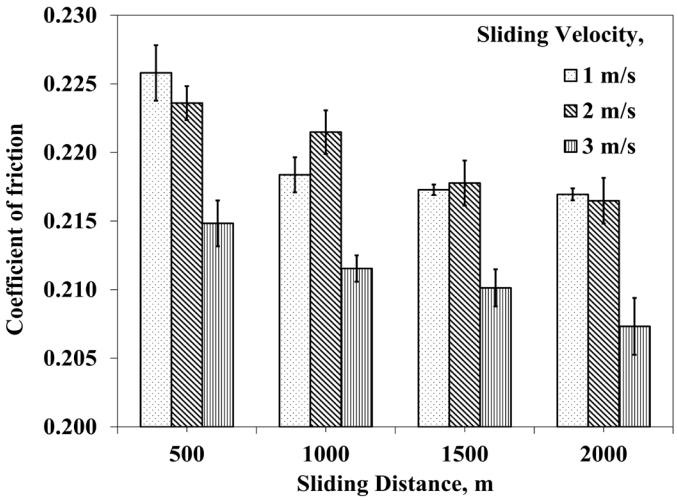

Fig. 9. Coefficient of friction with respect to varying sliding velocity at 29.43 N load

3.4. Wear mechanism

Analysis of the worn pin surface of magnesium metal-metal composite explored the wear mechanisms involved during the dry sliding, and the mechanisms of adhesion, abrasion, thermal softening, oxidation, and delamination are observed.

3.4.1. Abrasion

Abrasive wear occurs due to the contact of hard asperities during relative motion, resulting in micro-cutting and fatigue over the soft and ductile materials. The worn surface image of the pin at 9.81 N load and 1 m/s sliding velocity is shown in Fig. 10, which shows the existence of several grooves along with the marks of the plough in the direction of sliding. Similarly, grooves and ploughs along the direction of sliding were observed in the worn surface of pins under the 9.81 N load with all sliding velocities and at 19.62 N load with 1 and 2 m/s sliding veloci-

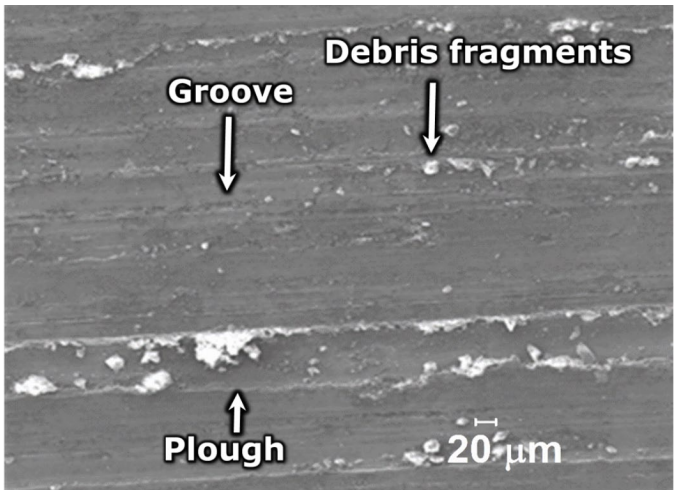

Fig. 10. Worn surface for 9.81 N load and 1 m/s sliding velocity exploring abrasion mechanism

ties [42]. The reason for the generation of grooves and ploughs is due to the impact of micro-cutting by the contact of sharp asperities and micro fatigue by the contact of blunt asperities, respectively, as the magnesium is low strength and high plastic in nature as observed elsewhere [31,32,43,44]. Although there was a material removal through abrasion at the initial stages, further sliding of a pin ended in transforming mechanisms such as softening and melting, diminishing the significant appearance of grooves. The effect of micro-cutting results in debris formation in the form of ribbons and a similar type of ribbon is observed in the collected wear debris shown in Fig. 11. Further, the micro-examination of wear debris shows that the ribbon strips were twinned with themselves and that there were stacked ribbons with more than one layer.

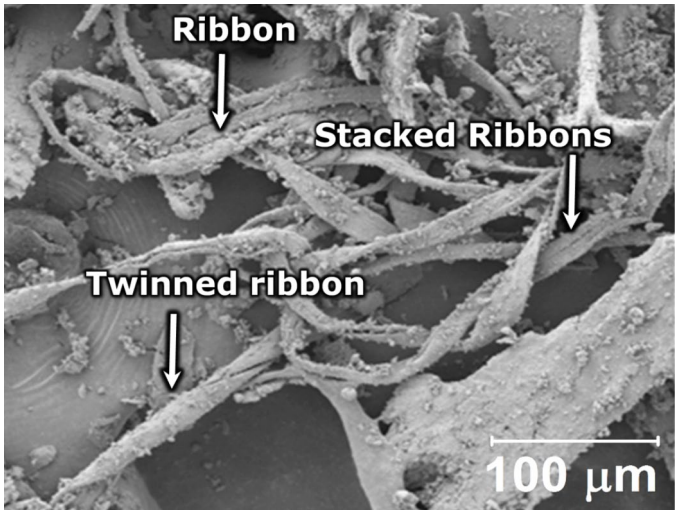

Fig. 11. Wear debris obtained for 9.81 N load and 1 m/s sliding velocity showing ribbon strips

3.4.2. Thermal softening

Due to the continuous action of loading and sliding, the temperature of sliding pairs increased, making the material soften and transform into a plastic state. Then, the softened material is pulled or wiped away due to the action of sliding, accumulating at pin ends [37], which is termed thermal softening. At higher load and higher sliding velocity, extruded layers at the corners of wear pins are similar to the observation reported by An et al. [45]. The worn surface of the pin for 29.43 N load and 3 m/s sliding velocity is shown in Fig. 12, which shows the deposition of wiped materials in the form of segregated layers accumulated at the ends of the wear pin. The thermal softening mechanism left out the wear debris as thin flakes or large sheets, which convey the transition from mild to severe wear. The wear debris collected for 29.43 N load and 3 m/s sliding velocity shows the presence of large sheets and thin flakes, as shown in Fig. 13, which conveys the softening mechanism reported by Huang et al. [46]. Besides, the surface of wear debris is smooth with glazed layers, which expresses the thermal softening condition reported by Lim et al. and Nguyen et al. [47,48].

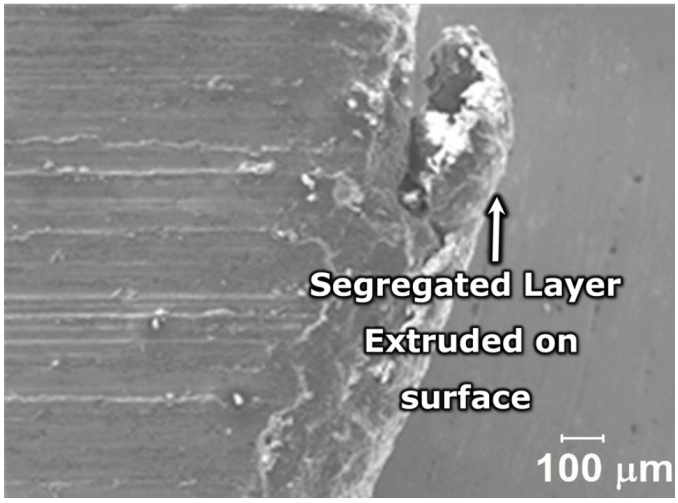

Fig. 12. Worn surface for 29.43 N load and 3 m/s sliding velocity exploring thermal softening and melting

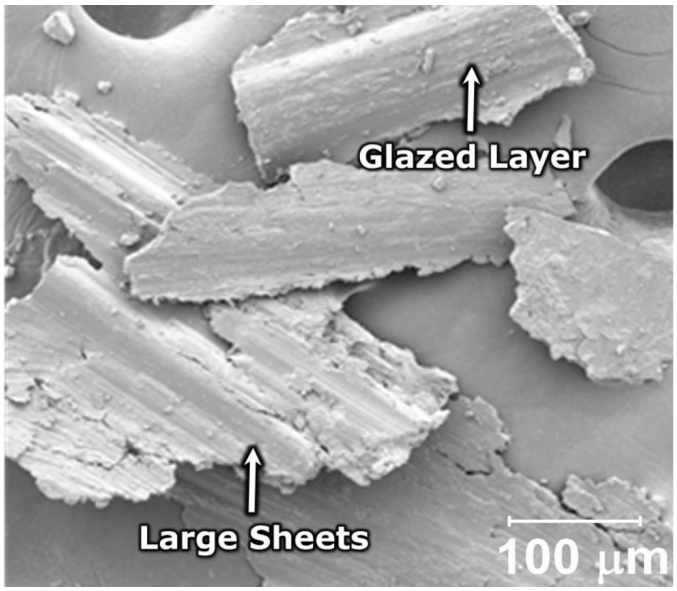

Fig. 13. Wear debris obtained for 29.43 N load and 3 m/s sliding velocity showing large sheets

3.4.3. Oxidation

The formation of the oxide layer on the pin surface due to the reaction with atmospheric oxygen is called oxidation, and the temperature directly influences the oxidation rate. The worn surface of the pin at 3 m/s sliding velocity at all load combinations exhibited the formation of oxidation. The worn surface of the pin for 29.43 N load and 3 m/s sliding velocity is shown in Fig. 14, shows the oxide formation, and it is confirmed with the elemental mapping, which shows the presence of oxygen content (embedded EDS map in Fig. 14). Also, the oxide formation over the pin surface is confirmed with the spectrum analysis, which shows the oxygen weight percentages as 55.99 and 55.74 at points 1 and 2, respectively. In the process of oxidation, a thin film of the oxide layer is formed in reaction with the atmospheric oxygen on the sliding surface due to the intense temperature rise

[49], and further sliding of the pin disintegrates the formed thin film layer into a fine powder of debris as reported by Turan et al. and Zhang et al. [31,32]. The wear debris collected for 29.43 N load and 3 m/s sliding velocity shows the fine powder debris, as shown in Fig. 15, confirms the oxidation mechanism.

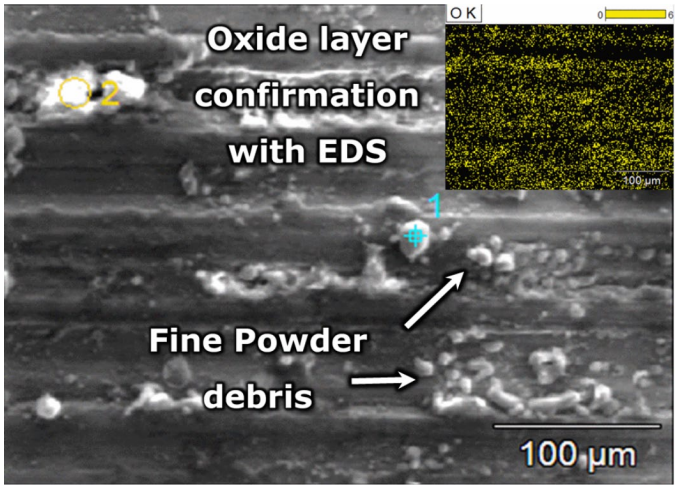

Fig. 14. Worn surface for 29.43 N load and 3 m/s sliding velocity exploring oxidation mechanism

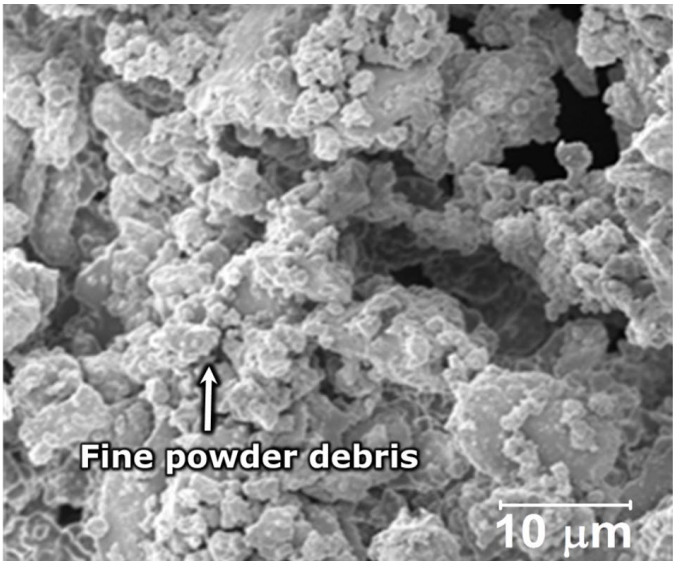

Fig. 15. Wear debris obtained for 29.43 N load and 3 m/s sliding velocity showing powders of debris

3.4.4. Delamination

Delamination is primarily based on dislocation theory, which is the fracture and deformation of materials plastically. During sliding, the hard asperities exert surface traction on the softer surface, which induces plastic deformation by means of shear. This deformation initiates the crack at the subsurface and further nucleates, resulting in the loss of worn-out particles as debris in the form of flakes [36,50,51]. At lower loading conditions, the samples unveiled traces of delamination on the worn surface. The worn surface for 9.81 N load and 3 m/s sliding velocity shown in Fig. 16 shows the existence of shallow craters due to the effect of delamination. The crater is 150 micrometres in length and 30 micrometres in width, with several steps down layers. The collected wear debris for 9.81 N load and 3 m/s sliding velocity shown in Fig. 17 shows the presence of large flakes and sheets, conveying the existence of a delamination mechanism as observed by Elleuch et al. [52]. Two large flakes are observed in Fig. 17; one is 110-micrometre length with 45 micrometres in width, and the other is 130 micrometres in length with 13 micrometres in width, which articulates the detachment of the first flake from the top layer of the crater and the second flake may show the subsequent detachment of debris from the shallow craters.

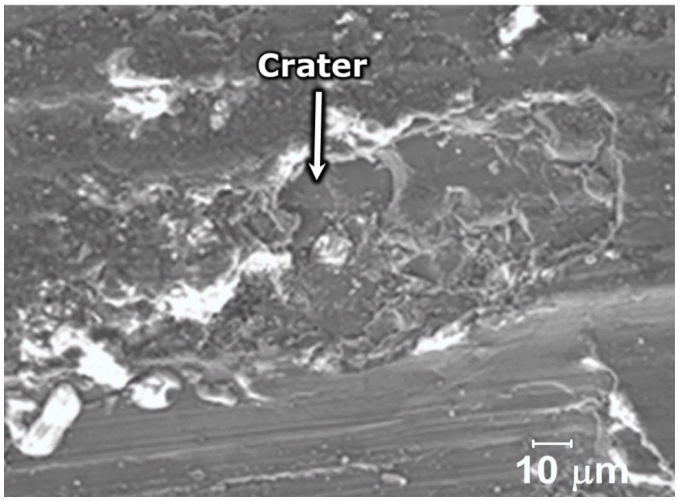

Fig. 16. Worn surface for pin at 9.81 N load and 3 m/s sliding velocity exploring delamination mechanism

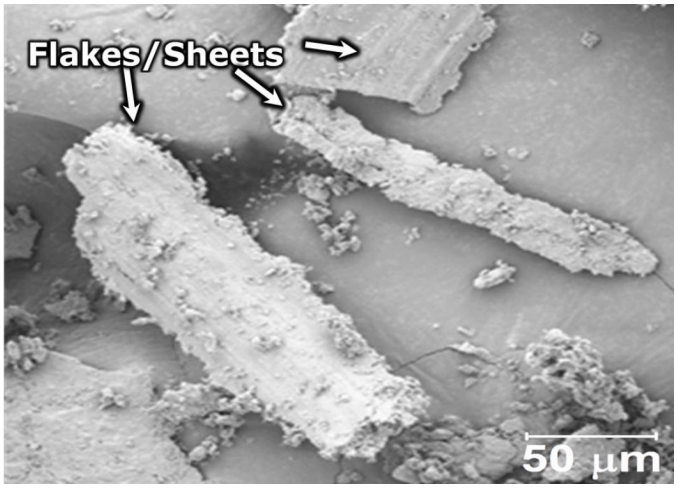

Fig. 17. Wear debris obtained for 9.81 N load and 3 m/s sliding velocity showing flakes

3.4.5. Adhesion

The normal force acting on the wear pin and the relative motion during sliding made the material softens, and an interface bond in terms of a micro-weld is formed between the soft mate-

rial and hard material [31]. Further, the relative motion induces the shear force, which leads to the peel of the adhesive bond in the direction of sliding from the softer material as it seems to be weaker. The dominance of the adhesion mechanism is observed in combination with lower sliding velocity with medium and higher loads. The worn surface of the pin for 19.62 N load and 1 m/s sliding velocity is shown in Fig. 18, which shows the presence of deep ploughs due to the smear of adhesive layers, along with a crack perpendicular to the direction of sliding [37]. The wear debris for 19.62 N load and 1 m/s sliding velocity is shown in Fig. 19, which shows the wiped-out adhesive layer of debris with the formation of furrows in a row. This is evident in the occurrence of adhesion mechanism, and similar observations are reported elsewhere [37,44,47]. Also, the traces of thin adhesive film layers over the counter disc surface are observed due to material deformation, as observed by Elleuch et al. [52].

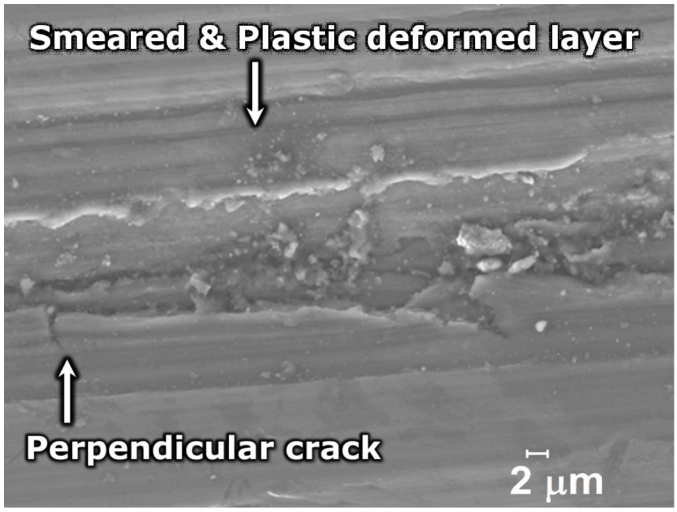

Fig. 18. Worn surface for 19.62 N load and 1 m/s sliding velocity exploring adhesion mechanism

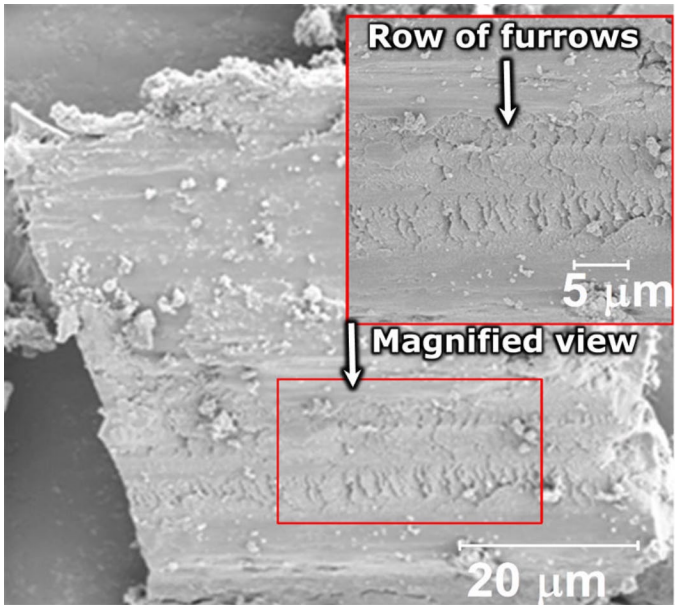

Fig. 19. Wear debris obtained for 19.62 N load and 1 m/s showing row of furrows

3.5. Wear mechanism summary

The influence of tribological parameters during the dry sliding of magnesium metal-metal composite is experimentally investigated and analysed. With the attained results, the mechanism involved in the tribological behaviour of the produced magnesium composite is displayed in TABLE 1 for better and easier understanding. Abrasion, adhesion, and delamination mechanisms dominate at lower load and lower sliding velocity. Further, an increase in sliding velocity induces the transformation in the mechanism by forming an oxide layer along with the adhesion mechanism. The increase in both the load and sliding velocity increases the force acting on the pin, which induces the metal-softening and melting of magnesium composite, which leads to a segregation of deformed layers protruding on the pin edges.

TABLE 1

Summary of wear mechanisms

Parameters	Wear mechanisms					
	Abrasion	Adhesion	Delamination	Melting	Oxidation	Softening
09.81 N, 1 m/s	√	√	√			
09.81 N, 2 m/s	√	√	√			
09.81 N, 3 m/s	√	√	√		√	√
19.62 N, 1 m/s	√	√	√			
19.62 N, 2 m/s		√		√	√	√
19.62 N, 3 m/s				√	√	√
29.43 N, 1 m/s	√	√	√	√		√
29.43 N, 2 m/s				√	√	√
29.43 N, 3 m/s				√	√	√

4. Conclusion

Using the disintegrating metal deposition approach, Metal-Metal Composite with particle reinforcement, 3 weight percent aluminum and 5.6 weight percent titanium was successfully developed. Metallurgical investigation revealed the presence of added particulates in a homogenous way. Further, the dry sliding wear test was conducted with the produced metal-metal composite by varying load and sliding velocity parameters. Almost all the increases in load and sliding velocity have a significant effect directly on the wear; the increase in sliding velocity results in a positive effect with a reduction in wear, and the increase in load results in a diverse effect with an increase in wear. The coefficient of friction is observed to increase with the increase in load. At lower and medium loads, the coefficient of friction is observed to increase from 1 m/s to 2 m/s sliding velocity, and then it decreases to 3 m/s sliding velocity. Meanwhile, the coefficient of friction decreases with increased sliding velocity for higher loads. The micro examinations on the worn surface

of wear pins and the collected debris particles helped reveal the mechanism involved in the wear. Abrasion, adhesion, oxidation, delamination, thermal softening, and melting are the identified mechanisms that dominate the dry sliding wear behaviour of the produced metal-metal composite.

REFERENCES

[1] Y.V.R.K. Prasad, K.P. Rao, S. Sasidhara, Hot Working Guide – A Compendium of Processing Maps (2015). DOI: https://doi.org/10.1016/B978-0-08-033454-7.50019-X

[2] L. Urtekin, R. Arslan, F. Bozkurt, Ü. Er, Investigation of tribological and mechanical properties of biodegradable az91 alloy produced by cold chamber high pressure casting method. Arch. Metall. Mater. **66**, 1, 205-216 (2021). DOI: https://doi.org/10.24425/amm.2021.134777

[3] K. Gobivel, K.S. Vijay Sekar, Machinability Studies on the Turning of Magnesium Metal Matrix Composites. Arch. Metall. Mater. **67**, 3, 939-948 (2022). DOI: https://doi.org/10.24425/amm.2022.139686

[4] S. Sankaranarayanan, S. Jayalakshmi, M. Gupta, Effect of addition of mutually soluble and insoluble metallic elements on the microstructure, tensile and compressive properties of pure magnesium. Mater. Sci. Eng. A **530**, 149-160 (2011). DOI: https://doi.org/10.1016/j.msea.2011.09.066

[5] S.F. Hassan, M. Gupta, Development of a novel magnesium–copper based composite with improved mechanical properties. Mater. Res. Bull. **37**, 2, 377-389 (2002). DOI: https://doi.org/10.1016/S0025-5408(01)00772-3

[6] S.F. Hassan, M. Gupta, Development of ductile magnesium composite materials using titanium as reinforcement. J. Alloys Compd. **345**, 246-251 (2002). DOI: https://doi.org/10.1016/S0925-8388(02)00413-9

[7] P. Pérez, G. Garcés, P. Adeva, Mechanical properties of a Mg-10 (vol.%)Ti composite. Compos. Sci. Technol. **64**, 145-151 (2004). DOI: https://doi.org/10.1016/S0266-3538(03)00215-X

[8] ASM International, Properties and Selection: Nonferrous Alloys and Special-Purpose Materials **2** (1990). DOI: https://doi.org/10.31399/asm.hb.v02.9781627081627

[9] X.D. Niu, D.Q. An, X. Han, W. Sun, T.F. Su, J. An, R.G. Li, Effects of Loading and Sliding Speed on the Dry Sliding Wear Behavior of Mg-3Al-0.4Si Magnesium Alloy. Tribol. Trans. **60**, 238-248 (2017). DOI: https://doi.org/10.1080/10402004.2016.1158890

[10] K.K. Ajith Kumar, U.T.S. Pillai, B.C. Pai, M. Chakraborty, Dry sliding wear behaviour of Mg-Si alloys. Wear. **303**, 56-64 (2013). DOI: https://doi.org/10.1016/j.wear.2013.02.020

[11] C. Taltavull, P. Rodrigo, B. Torres, A.J. López, J. Rams, Dry sliding wear behavior of AM50B magnesium alloy. Mater. Des. **56**, 549-556 (2014). DOI: https://doi.org/10.1016/j.matdes.2013.12.015

[12] J. An, R.G. Li, Y. Lu, C.M. Chen, Y. Xu, X. Chen, L.M. Wang, Dry sliding wear behavior of magnesium alloys. Wear **265**, 97-104 (2008). DOI: https://doi.org/10.1016/j.wear.2007.08.021

[13] S.C. Ram, K. Chattopadhyay, I. Chakrabarty, Effect of magnesium content on the microstructure and dry sliding wear behavior of centrifugally cast functionally graded A356-Mg 2 Si in situ composites Effect of magnesium content on the microstructure and dry sliding wear behavior of centrifugally cast. Mater. Res. Express. **5**, 4 (2018). DOI: https://doi.org/10.1088/2053-1591/aabbea

[14] M. Srinivasan, C. Loganathan, M. Kamaraj, Q.B. Nguyen, M. Gupta, R. Narayanasamy, Sliding wear behaviour of AZ31B magnesium alloy and nano-composite. Trans. Nonferrous Met. Soc. China (English Ed. **22**, 60-65 (2012). DOI: https://doi.org/10.1016/S1003-6326(11)61140-0

[15] P. Seenuvasaperumal, A. Elayaperumal, R. Jayavel, Influence of calcium hexaboride reinforced magnesium composite for the mechanical and tribological behviour. Tribol. Int. **111**, 18-25 (2017). DOI: https://doi.org/10.1016/j.triboint.2017.02.042

[16] J. An, Y.X. Zhang, X.X. Lv, Tribological Characteristics of Mg – 3Al – 0 . 4Si – 0 . 1Zn Alloy at Elevated Temperatures of 50–200°C,. Tribol. Lett. **66**, 1-17 (2018). DOI: https://doi.org/10.1007/s11249-017-0968-8

[17] X.D. Niu, D.Q. An, X. Han, W. Sun, T.F. Su, J. An, R.G. Li, D.Q. An, X. Han, W. Sun, T.F. Su, J. An, R.G.L. Effects, Effects of Loading and Sliding Speed on the Dry Sliding Wear Behavior of Mg-3Al-0.4Si Magnesium Alloy. Tribol. Trans. **60**, 238-248 (2017). DOI: https://doi.org/10.1080/10402004.2016.1158890

[18] D. Mandal, L. Murmu, C. Choudhary, G. Singh, Influence of alloying elements and grain refiner on microstructure, mechanical and wear properties of Mg-Al-Zn alloys. Can. Metall. Q. 1-11(2018). DOI: https://doi.org/10.1080/00084433.2018.1540087

[19] G. Germen, G. Yarkadaş, H. Şevik, Influence of strontium addition on the wear behavior of Mg-3Al-3Sn alloys produced by gravity casting. Mater. Test. **57**, 997-1000 (2015). DOI: https://doi.org/10.3139/120.110806

[20] V. Kavimani, K.S. Prakash, T. Thankachan, Experimental investigations on wear and friction behaviour of SiC@r-GO reinforced Mg matrix composites produced through solvent-based powder metallurgy. Compos. Part B Eng. **162**, 508-521 (2019). DOI: https://doi.org/10.1016/j.compositesb.2019.01.009

[21] ASM International, Metallography and Microstructures (2004). DOI: https://doi.org/10.31399/asm.hb.v09.9781627081771

[22] S. Baskaran, V. Anandakrishnan, M. Duraiselvam, Investigations on dry sliding wear behavior of in situ casted AA7075-TiC metal matrix composites by using Taguchi technique. Mater. Des. **60**, 184-192 (2014). DOI: https://doi.org/10.1016/j.matdes.2014.03.074

[23] C. Saravanan, V. Subramanian, K. Anandakrishnan, S. Sathish, Tribological behavior of AA7075-TiC composites by powder metallurgy. Ind. Lubr. Tribol. **70**, 1066-1071 (2018). DOI: https://doi.org/10.1108/ILT-10-2017-0312

[24] American Society for Testing and Materials, ASTM G99-17: Standard Test Method for Wear Testing with a Pin-on-Disk Apparatus. (2017). DOI: https://doi.org/10.1520/G0099-17.Copyright.

[25] S. Sathish, V. Anandakrishnan, S. Sankaranarayanan, M. Gupta, Optimization of wear parameters of magnesium metal-metal composite using Taguchi and GA technique. J. Tribol. **23**, 76-89 (2019).

[26] S. Sathish, V. Anandakrishnan, M. Gupta, Analysis of Wear Behavior of a Novel Magnesium Metal-Metal Composite. Surf. Rev. Lett. **27** (2020).
DOI: https://doi.org/10.1142/S0218625X19502287

[27] A. Manjunath, V. Anandakrishnan, S. Ramachandra, K. Parthiban, S. Sathish, Optimization of Tribological Parameters of Pre-Positioned Wire Based Electron Beam Additive Manufactured Ti-6Al-4V Alloy. Arch. Metall. Mater. **67**, 2, 447-454 (2022).
DOI: https://doi.org/10.24425/amm.2022.137776

[28] Z.R. Yang, S.Q. Wang, Y.T. Zhao, M.X. Wei, Evaluation of wear characteristics of Al3Tip/Mg composite. Mater. Charact. **61**, 554-563 (2010).
DOI: https://doi.org/10.1016/j.matchar.2010.02.014

[29] B. Çiçek, H. Ahlatçi, Y. Sun, Wear behaviours of Pb added Mg-Al-Si composites reinforced with in situ Mg2Si particles. Mater. Des. **50**, 929-935 (2013).
DOI: https://doi.org/10.1016/j.matdes.2013.03.097

[30] W. Yu, H. Zhao, X. Hu, Anisotropic mechanical and physical properties in textured Ti2AlC reinforced AZ91D magnesium composite. J. Alloys Compd. **732**, 894-901 (2018).
DOI: https://doi.org/10.1016/j.jallcom.2017.10.255

[31] M.E. Turan, Y. Sun, Y. Akgul, Mechanical, tribological and corrosion properties of fullerene reinforced magnesium matrix composites fabricated by semi powder metallurgy. J. Alloys Compd. **740**, 1149-1158 (2018).
DOI: https://doi.org/10.1016/j.jallcom.2018.01.103

[32] L. Zhang, X. Luo, J. Liu, Y. Leng, L. An, Dry sliding wear behavior of Mg-SiC nanocomposites with high volume fractions of reinforcement. Mater. Lett. **228**, 112-115 (2018).
DOI: https://doi.org/10.1016/j.matlet.2018.05.114

[33] R.V. Prasad, D. Jeyasimman, G. Parande, M. Gupta, R. Narayanasamy, Investigation on dry sliding wear behavior of Mg / BN nanocomposites. J. Magnes. Alloys **6**, 263-276 (2018).
DOI: https://doi.org/10.1016/j.jma.2018.05.005

[34] M. Habibnejad-korayem, R. Mahmudi, H.M. Ghasemi, W.J. Poole, Tribological behavior of pure Mg and AZ31 magnesium alloy strengthened by Al2O3 nano-particles. Wear **268**, 405-412 (2010).
DOI: https://doi.org/10.1016/j.wear.2009.08.031

[35] M.E. Turan, Y. Sun, Y. Akgul, Y. Turen, H. Ahlatci, The effect of GNPs on wear and corrosion behaviors of pure magnesium. J. Alloys Compd. **724**, 14-23 (2017).
DOI: https://doi.org/10.1016/j.jallcom.2017.07.022

[36] S. Wen, P. Huang, Principles of Tribology (2017).
DOI: https://doi.org/0.1002/9781119214908

[37] H.J. Hu, Z. Sun, Z.W. OU, X.Q. Wang, Wear behaviors and wear mechanisms of wrought magnesium alloy AZ31 fabricated by extrusion-shear. Eng. Fail. Anal. **72**, 25-33 (2017).
DOI: https://doi.org/10.1016/j.engfailanal.2016.11.014

[38] N. Li, H. Yan, The Effects of Rare Earth Pr and Heat Treatment on the Wear Properties of AZ91 Alloy. Crystals **8**, 6, 256 (2018).
DOI: https://doi.org/10.3390/cryst8060256

[39] A. Kumar, T. Staedler, X. Jiang, Effect of normal load and roughness on the nanoscale friction coefficient in the elastic and plastic contact regime. Beilstein J. Nanotechnol. **4**, 66-71 (2013).
DOI: https://doi.org/10.3762/bjnano.4.7

[40] D. Kakaš, B. Škorić, S. Mitrović, M. Babić, P. Terek, A. Miletić, M. Vilotić, Influence of load and sliding speed on friction coefficient of IBAD deposited TiN. Tribol. Ind. **31**, 3-10 (2009).

[41] Y. Ando, Decrease in friction coefficient under extremely low load. Tribol. Ser. **32**, 533-54 (1997).
DOI: https://doi.org/10.1016/S0167-8922(08)70480-2

[42] K. Kaur, O.P. Pandey, Dry sliding wear behavior of zircon sand reinforced Al-Si alloy. Tribol. Lett. **38**, 377-387 (2010).
DOI: https://doi.org/10.1007/s11249-010-9620-6

[43] X. Zhou, Y. Gao, Y. Wang, Wear behavior of Ni-coated carbon fiber and ZrC particles reinforced 2024Al matrix composites. Wear **528-529**, 204967 (2023).
DOI: https://doi.org/10.1016/j.wear.2023.204967

[44] X. Zhou, Y. Gao, Y. Wang, P. Xiao, X. Huang, Effects of ZrC particles, load and sliding speed on the wear behavior of the ZrC/2024Al composites. Wear **506-507**, 204465 (2022).
DOI: https://doi.org/10.1016/j.wear.2022.204465

[45] J. An, W. Sun, X.D. Niu, Dry Sliding Wear Behavior and a Proposed Criterion for Mild to Severe Wear Transition of Mg–3Al–0.4Si–0.1Zn Alloy. Tribol. Lett. **65** (2017).
DOI: https://doi.org/10.1007/s11249-017-0882-0

[46] S.J. Huang, Y.R. Jeng, V.I. Semenov, Y.Z. Dai, Particle size effects of silicon carbide on wear behavior of SiC p-reinforced magnesium matrix composites. Tribol. Lett. **42**, 79-87 (2011).
DOI: https://doi.org/10.1007/s11249-011-9751-4

[47] C.Y.H. Lim, S.C. Lim, M. Gupta, Wear behaviour of SiCp-reinforced magnesium matrix composites. Wear **255**, 629-637 (2003). DOI: https://doi.org/10.1016/S0043-1648(03)00121-2

[48] Q.B. Nguyen, Y.H.M. Sim, M. Gupta, C.Y.H. Lim, Tribology characteristics of magnesium alloy AZ31B and its composites. Tribol. Int. **82**, 464-471 (2015).
DOI: https://doi.org/10.1016/j.triboint.2014.02.024

[49] L. Falcon-Franco, E. Bedolla-Becerril, J. Lemus-Ruiz, J.G. Gonzalez-Rodríguez, R. Guardian, I. Rosales, Wear performance of TiC as reinforcement of a magnesium alloy matrix composite. Compos. Part B Eng. **42**, 275-279 (2011).
DOI: https://doi.org/10.1016/j.compositesb.2010.11.012

[50] N.P. Suh, An overview of the delamination theory of wear. Wear **44**, 1-16 (1977).
DOI: https://doi.org/10.1016/0043-1648(77)90081-3

[51] S.K. Jo, W.J. Lee, Y.H. Park, I.M. Park, Effect of SiC particle size on wear properties of Al2O3.SiO2/SiC/Mg hybrid metal matrix composites. Tribol. Lett. **45**, 101-107 (2012).
DOI: https://doi.org/10.1007/s11249-011-9866-7

[52] R. Elleuch, K. Elleuch, R. Mnif, V. Fridrici, P. Kapsa, G. Khélifati, Comparative study on wear behaviour of magnesium and aluminium alloys. Proc. Inst. Mech. Eng. Part J: J. Eng. Tribol. **220**, 479-486 (2006). DOI: https://doi.org/10.1243/13506501jet70